Molecular Mechanisms Mediating the Effect of Mono-(2-Ethylhexyl) Phthalate on Hormone-Stimulated Steroidogenesis in MA-10 Mouse Tumor Leydig Cells

Jinjiang Fan, Kassim Traore, Wenping Li, Hakima Amri, Hongzhan Huang, Cathy Wu, Haolin Chen, Barry Zirkin, and Vassilios Papadopoulos

The Research Institute of the McGill University Health Centre (J.F., V.P.) and Departments of Medicine (J.F., V.P.), Biochemistry (V.P.), Pharmacology & Therapeutics (V.P.), McGill University, Montreal, Quebec, Canada H3G 1A4; Departments of Biochemistry and Molecular and Cellular Biology (K.T., W.L., H.A., H.H., C.W., V.P.) and Physiology and Biophysics (H.A.), Georgetown University Medical Center, Washington, D.C. 20057; and Department of Biochemistry and Molecular Biology (K.T., H.C., B.Z.), Johns Hopkins University Bloomberg School of Public Health, Baltimore, Maryland 21205

Di-(2-ethylhexyl) phthalate, a widely used plasticizer, and its active metabolite, mono-(2-ethylhexyl) phthalate (MEHP), have been shown to exert adverse effects on the reproductive tract in developing and adult animals. As yet, however, the molecular mechanisms by which they act are uncertain. In the present study, we address the molecular and cellular mechanisms underlying the effects of MEHP on basal and human chorionic gonadotropin (hCG)-stimulated steroid production by MA-10 Leydig cells, using a systems biology approach. MEHP induced dose-dependent decreases in hCG-stimulated steroid formation. Changes in mRNA and protein expression in cells treated with increasing concentrations of MEHP in the presence or absence of hCG were measured by gene microarray and protein high-throughput immunoblotting analyses, respectively. Expression profiling indicated that low concentrations of MEHP induced the expression of a number of genes that also were expressed after hCG stimulation. Cross-comparisons between the hCG and MEHP treatments revealed two genes, *Anxa1* and *AR1*. We suggest that these genes may be involved in a new self-regulatory mechanism of steroidogenesis. The MEHP-induced decreases in hCG-stimulated steroid formation were paralleled by increases in reactive oxygen species generation, with the latter mediated by the *Cyp1a1* gene and its network. A model for the mechanism of MEHP action on MA-10 Leydig cell steroidogenesis is proposed. (*Endocrinology* **151:** 3348–3362, 2010)

Human exposures to endocrine disruptors have the potential to lead to cryptorchidism, hypospadias, testicular cancer, and poor semen quality (1). During mammalian sex differentiation, androgen play a critical role in programming organ morphogenesis and neural function (2). At all developmental stages, androgens exert effects that are immediate, multiple, reversible, and dose dependent, and thus their presence in sufficient amounts is a critical determinant of the male phenotype (2). Consequently, environmental chemicals that alter endocrine function pose potential risks to the reproductive health of humans and wildlife (3).

The phthalic acid esters are used as plasticizers in manufacturing polyvinyl chloride and other plastics. Phthalates, such as di-(2-ethylhexyl) phthalate (DEHP), are loosely held between the interstices of the polymer matrix and thus are ubiquitous contaminants of the environment (4). Human exposures to DEHP via ingestion, inhalation, and dermal contact result in measurable levels of DEHP and metabolites in blood, urine, semen, breast milk, and umbilical cord blood (5–11). Normal human exposure to DEHP can be 3–30 μg/kg · d and as high as 10–20 mg/kg · d via neonate transfusion or parenteral nutrition (12–14).

Abbreviations: Anxa1, Annexin A1; AR, androgen receptor; DCFH-DA, 2′,7′-dichlorofluorescin diacetate; DEHP, di-(2-ethylhexyl) phthalate; hCG, human chorionic gonadotropin; mAb, monoclonal antibody; MEHP, mono-(2-ethylhexyl) phthalate; MTT, 3-(4,5-dimethylthiazol-2-yl)-2,5-diphenyl tetrazolium bromide; NAC, N-acetylcysteine; PPAR, proliferator-activated receptor; Q-PCR, quantitative PCR; ROS, reactive oxygen species.

DEHP has been shown to cause reproductive toxicity in both developing and adult animals. DEHP is found in the amniotic fluid, placenta, and fetal tissues of rats after its ingestion by pregnant dams (15, 16). Fetal exposures to DEHP have been shown to result in reduced litter size, cryptorchidism, and, later in life, Leydig cell hyperplasia, testicular atrophy, reduced serum levels of serum testosterone, and reduced fertility (1, 18 –20). In various tissues and cells, the DEHP active metabolite mono-(2-ethylhexyl) phthalate (MEHP) is responsible for the adverse health effects associated with phthalate exposure (21). The detrimental effects of DEHP administration on the male reproductive tract also have been attributed to MEHP (22). For example, MEHP was shown to inhibit LH-stimulated steroid formation by both purified adult rat Leydig cells and MA-10 mouse tumor Leydig cells (23–25). The mechanism by which MEHP functions to alter steroidogenesis is uncertain.

In the present study, we address the possible mechanism(s) by which MEHP affects MA-10 Leydig cell steroidogenesis by examining MEHP effects on progesterone formation, gene and protein expression profiling, pathway mapping, and reactive oxygen species (ROS) production. Gene and protein expression were measured using GeneChip (26) and PowerBlot (27) analyses, and real-time quantitative PCR (Q-PCR) was used to confirm the gene array findings. Data obtained were mapped to oxidative stress and steroid biosynthesis pathways. The results presented herein suggest a new mechanism of MEHP action on Leydig cell steroidogenesis via *Cyp1a1*-mediated ROS stress.

Materials and Methods

Cell culture and treatments

MA-10 cells were grown in DMEM/nutrient mixture F-12 Media, supplemented with 2.5% horse and 5% fetal bovine serum. Cells were grown to subconfluence, incubated with MEHP (Sigma-Aldrich, St. Louis, MO) for 16, 24, or 48 h, washed with serum-free medium, and incubated for 2 h in the presence or absence of a saturating concentration of human chorionic gonadotropin (hCG) (CR-125, 50 ng/ml; National Institute of Diabetes and Digestive and Kidney Diseases, Bethesda, MD). Media were collected for progesterone measurement, and cells were saved for examining ROS generation, protein determination, RNA isolation, and immunoblot analysis.

For some experiments, adult Sprague Dawley rat testis Leydig cells of 75–85% purity were prepared by collagenase dissociation followed by Percoll gradient centrifugation (28). Leydig cells were incubated with MEHP for 24 h, after which the cells were washed and stimulated for 2 h with hCG (50 ng/ml) in serum-free medium. Media were collected for testosterone measurements and cells for protein determination.

Steroid quantification

Progesterone production by MA-10 cells and testosterone production by rat Leydig cells were measured by RIA (24, 28, 29).

Analysis of cell viability

The effect of MEHP on cell viability was assessed with the 3-(4,5-dimethylthiazol-2-yl)-2,5-diphenyl tetrazolium bromide (MTT) cell viability/cytotoxicity assay (30).

Oligonucleotide microarray

The Affymetrix Murine Genome U74A version 2 GeneChip (26), which represents all sequences (~6000) in the mouse UniGene database (Build 74) plus approximately 2000 expressed sequence tagged clusters, was used to delineate profile changes in gene-expression in response to MEHP. After incubation of MA-10 cells with 0–10 μM MEHP for 24 h followed by incubation with or without hCG (50 ng/ml) for 2 h, the cells were used for total RNA isolation. Experiments were repeated three times, and RNA collected from the three separate experiments was amplified and biotinylated using the Affymetrix (Santa Clara, CA) protocol as described previously (26). Biotinylated cRNA was purified, fragmented, and hybridized to the arrays. After washing, the arrays were stained with streptavidin-phycoerythrin, enhanced with anti-streptavidin antibody, and then scanned with a confocal scanner (26). Image data were analyzed using the MicroArray Suite 5.0 Gene Expression analysis program (Affymetrix). The data were normalized, filtered, and subjected to cluster analysis.

High-throughput Western blot screening and data analysis

Primary screening was performed by BD Biosciences Transduction Laboratories (Lexington, KY) using the PowerBlot assay (27, 31) to determine the expression levels of 860 signal-transducing proteins. Briefly, after treatment of MA-10 cells with 1 μM MEHP for 48 h and 50 ng/ml hCG for 2 h, protein extracts containing total cellular protein were separated on 5–15% SDS-PAGE gradients and transferred onto nitrocellulose membranes. The membranes then were divided into 40 lanes using a chamber-forming grid. Individual lanes were incubated with a blend of monoclonal antibodies (mAbs). A total of 860 individual mAbs were used in the assay. A secondary goat antimouse horseradish peroxidase was used to visualize mAbs. Chemiluminescence data were captured by a charge-coupled device camera and quantified by computerized processing. Data were normalized to the total intensity value of all pixels in an image multiplied by 1,000,000. Ratios were calculated to express increases or decreases in protein expression. This study was repeated three times, and values were averaged.

Real-time Q-PCR

MA-10 cells were incubated with MEHP for 24 h and then with or without hCG for 2 h. After washing the cells, total RNA was isolated (32). Genomic DNA contamination was removed by RNase-free DNase digestion. Q-PCR was performed using the ABI PRISM 7700 Sequence Detector (Applied Biosystems, Foster City, CA) (32). PCR products were detected by measuring increase in fluorescence caused by the binding of SYBR Green I dye to double-stranded DNA. The comparative cycle threshold (C_T) method was used to analyze the data. The expression of

mRNA corresponding to a target gene was normalized to the endogenous reference 18S rRNA or hypoxanthine phosphoribosyltransferase for *Cyp1a1*. Three independent experiments were performed, each in triplicate. The forward and reverse primers used are listed in Supplemental Table 1 (published on The Endocrine Society's Journals Online web site at http://endo.endojournals.org).

Dose-response analysis

The microarray data were globally normalized, and linearity was confirmed before the consecutive sampling method was applied based on equivalence of the SD derived from the individual genes and SD derived from the consecutive samples (33, 34). Briefly, in two-array comparisons, the genes are ordered according to mean signal intensity and grouped in bins containing n consecutive genes (n = 25). The SD was calculated for each bin, and the SD function in linear approximation was determined by regression. Subsequently, specific probability intervals were evaluated so that the distance of corresponding points at upper and lower boundaries measured in SDs was invariant.

The candidate genes for the concentrations of 1, 3, and 10 μM MEHP were selected among the genes beyond the 0.95 probability interval using the requirement that they must lie outside the interval compared with control as well as the lowest (0.3 μM) MEHP dose. The candidates for the lowest concentration comparisons and comparison of MEPH *vs.* MEPH plus hCG were the genes above and below the 0.975 probability interval. To further assist in the evaluation of significance of the observed differences, we performed *t* test and *t* test with Bonferroni's correction, based on the similarity between the microarray distributions and theoretical *t* distribution at the degree of freedom equal to 12 (34). Heat maps were prepared using Heatmap Builder (version 1) (35). The genes used for the heat maps are those from the dose-response tables with the following two additional requirements: four coincidences and conformity with the dose-response curves, allowing for one exception.

Cluster and GenMAPP analysis

Clustering was performed using a self-organizing map algorithm to determine physiologically relevant patterns of gene expression via Genesis (36). Hierarchical cluster analysis on differentially expressed genes was performed using average linkage and correlation in GenePattern (version 3.1.1.) (37). Differential expression was determined using up or down changes of more than 2-fold. ROS pathways, steroid biosynthesis pathways, and the *Cyp1a1* gene network were evaluated for differential regulation using the visualization tool GenMAPP (38). We imported the whole gene set of the microarray into the program and used GenMAPP to illustrate pathways containing differentially expressed genes.

Measurement of ROS generation by 2′,7′-dichlorofluorescin diacetate-derived fluorescence

ROS generation by MA-10 cells in response to MEHP was assessed using 2′,7′-dichlorofluorescin diacetate (DCFH-DA)-derived fluorescence, as described previously (39). In brief, samples of 1×10^6 cells were incubated with DCFH-DA (10 μM) in the presence of MEHP or dimethylsulfoxide (vehicle) for 16 h. After cells were washed three times in PBS, the fluorescence intensity of cells in each sample was determined by fluorescence-activated cell sorting-scan analysis. Data were analyzed using

Cellquest software (BD Biosciences, Bedford, MA). ROS production by individual cells was visualized by incubating the cells with DCFH-DA and then examining 4′,6-diamidino-2-phenylindole-stained cells by fluorescence microscopy over time.

Statistics

Multiple means were compared using one-way ANOVA (Prism version 3.0; GraphPad Software, San Diego, CA). All *P* values are provided in the text or figure legends.

Results

Effect of MEHP on hCG-stimulated steroid production

As seen in Fig. 1A, incubation of MA-10 cells with MEHP (0.3–10 μM) for 24 or 48 h inhibited hCG-stimu-
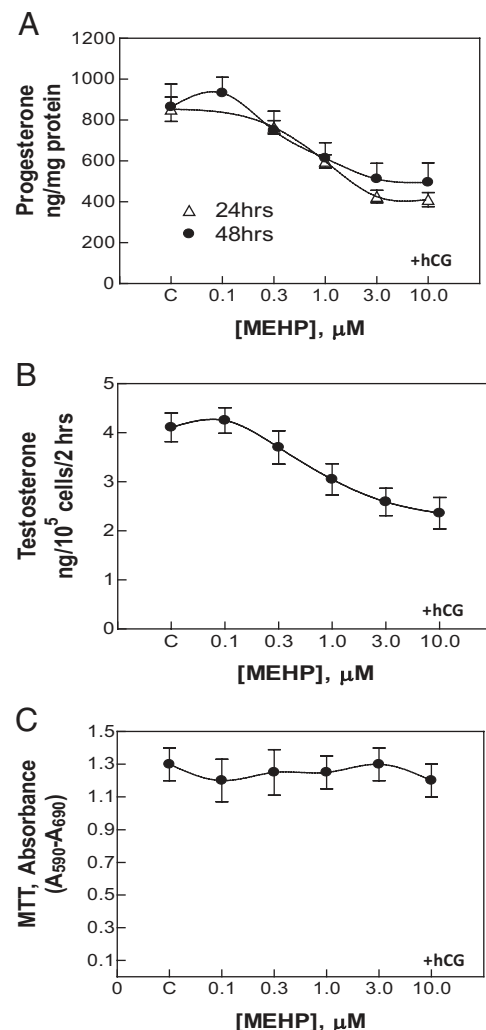
FIG. 1. Dose-response effects of MEHP on steroid synthesis by MA-10 Leydig tumor cells (A) and rat Leydig cells (B) and on mitochondrial functional integrity as assessed by the MTT assay (C). Cells were incubated in the absence (C) or presence of 0.1–10.0 μM MEHP for 24 or 48 h and with hCG (50 ng/ml) for 2 h. Mean $\pm$ SD (n = 16 for 24 h; n = 24 for 48 h). Significant inhibition of hCG-stimulated steroid formation was seen at 0.3–10 μM MEHP for 24 or 48 h ($P < 0.001$).

lated progesterone production significantly; with a 48 h incubation, the IC_{50} value was less than 1 μM. We also determined the effect of MEHP on testosterone production by Leydig cells isolated from the adult rat testis. Figure 1B shows that a 24-h exposure to MEHP (0.3–10 μM) inhibited hCG-stimulated testosterone production significantly, also with an IC_{50} value of less than 1 μM. Interestingly, at the 0.1 μM MEHP concentration, a slight increase in steroid production was seen in both MA-10 and rat Leydig cells (Fig. 1, A and B). At concentrations as high as 300 μM, MEHP (48-h exposure) was not toxic to the MA-10 cells (or to primary Leydig cells; data not shown) as assessed by MTT measurement (Fig. 1C).

Profiling of MEHP response genes by oligonucleotide array, dose-response, and cluster analyses

Affymetrix GeneChip microarrays were used to determine the effect of MEHP on mRNA expression. Among the approximately 6000 full-length genes and 2000 expressed sequence tagged clusters examined, those changes of 1.8-fold or greater compared with controls were further analyzed using self-organizing maps (Supplemental Fig. 1, A and B, Tables 2 and 3). Using hierarchical cluster analysis, overall patterns of expression of the 8000 genes were grouped into five distinct clusters (Supplemental Fig. 2). Genes in the first cluster, referred to as hCG-independent/MEHP-induced, were up-regulated by low-dose MEHP (0.3 μM) independently of hCG. Genes of the second cluster (hCG-independent/MEHP-induced) were up-regulated in response to increasing MEHP dose from 0.3 to 10 μM, also independently of hCG. Indeed, in the case of these genes, the induction of MEHP appeared to be repressed when the cells were treated with MEHP and hCG. Genes of the third group, referred to as hCG-dependent/MEHP-induced, were up-regulated increasingly by increasing MEHP dose, but only when the cells also were treated with hCG. Among these, some genes responded to MEHP at a high dose (hCG-dependent/MEHP-induced) and others to MEHP at a low dose.

Additional analysis revealed that 35 genes were up-regulated and 11 genes down-regulated by MEHP treatment alone (Fig. 2A). Among the up-regulated genes were transcription factors involved in ROS metabolism, including Fos and junB. These genes are considered to be major components of activator protein-1, a redox-sensitive transcription factor complex (40). Other up-regulated genes included *Cyp2C39*, involved in retinoic acid 4-hydroxylation via aryl hydrocarbon receptor (41), peroxisome proliferator-activated receptor γ (PPARγ) binding protein, involved in important signaling pathways (42), and PTC7 protein phosphatase homolog (mouse ortholog of

human T-cell activation protein phosphatase 2C), a member of a new PP2CR subfamily (43). Down-regulated genes included male enhanced antigen 1, related to testicular morphogenesis (44). As shown in Fig. 2B, MEHP plus hCG treatment induced the expression of 13 genes and the repression of 24 genes. Among the repressed genes was annexin A1 (*Anxa1*), a key player in the physiology and pharmacology of glucocorticoid hormones and drugs (45, 46). This could have significance for the regulation of steroid generation and antiinflammatory action (see below). Supplemental Tables 4–7 show the effects of MEHP alone *vs.* MEHP plus hCG using less strict selection criteria.

Comparison of Affymetrix array and Q-PCR data

Q-PCR was used selectively to confirm changes in gene expression shown by the Affymetrix array. Supplemental Fig. 3A shows the mRNA expression patterns of 13 genes detected by the Affymetrix array, and Supplemental Fig. 3B shows the mRNA expression patterns of these same genes obtained by Q-PCR. For this study, the MA-10 cells were incubated with increasing concentrations of MEHP alone for 24 h (shown as control C, 0.3–10.0 μM), or with MEHP and then hCG for 2 h (shown as C+, 0.3–10.0 μM +). In all cases, the Q-PCR data were consistent with the results obtained by Affymetrix array. Statistical analysis of the Q-PCR results (Supplemental Fig. 3B) confirmed that the decreased mRNA expressions of *Clk*, *Dld*, *Msh2*, *Xpol*, *Zfp97*, *Tspo*, *StAR*, and *Stat6* as seen by Affymetrix analysis of cells treated with MEHP plus hCG (Supplemental Fig. 3A) in fact represented statistically significant decreases ($P < 0.001$ for *Clk*, *Dld*, *Msh2*, *Xpol*, and *Zfp97*; $P < 0.01$ for *StAR*; and $P < 0.05$ for *Tspo* and *Stat6*). The increases seen by Affymetrix array in *Egr1*, *Nr4a1*, *P160*, and *Pdcd6* mRNA ($P < 0.001$ for *Egr1*; $P < 0.001$ for *Nr4a1* and *P160*; $P < 0.01$ for *Pdcd6*) also were significant. Q-PCR also confirmed increases in genes in response to MEHP alone ($P < 0.001$ for *Egr1* and *Nr4a1*; $P < 0.001$ for *P160*; $P < 0.01$ for *Pdcd6*; $P < 0.05$ for *JunB* mRNA).

High-throughput immunoblot identification of MEHP response genes

Total cellular protein isolated from MEHP-treated and control MA-10 cells was submitted to high-throughput analysis using PowerBlot. A semiquantitative value representing the general trend of protein changes was used to analyze protein levels in MEHP-treated cells relative to control. Based on the confidence with which the identity of the protein could be deduced, we separated the bands into five groups (Supplemental Tables 8 and 9). Supplemental Table 8 summarizes the proteins that responded when MA-10 cells were exposed to 1 μM MEHP alone for
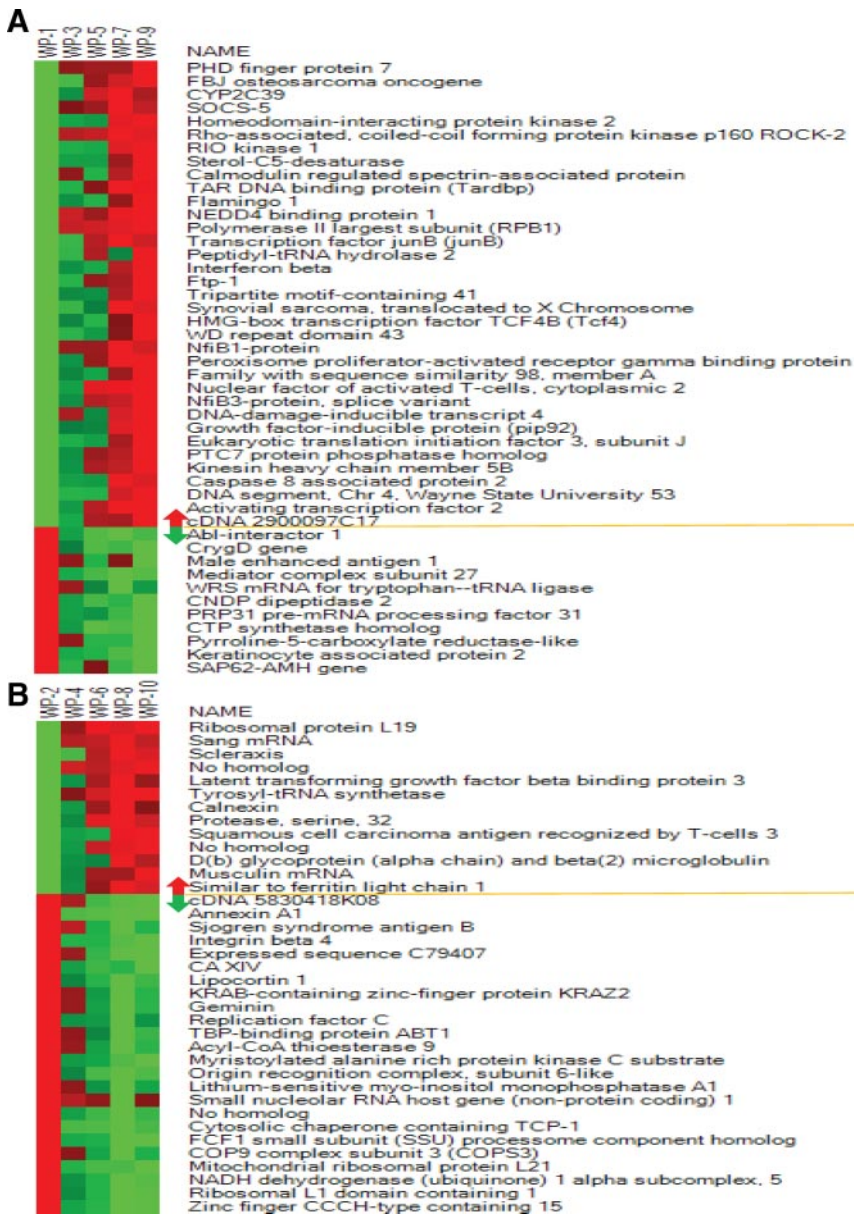
FIG. 2. Heat map showing the expression of MA-10 mouse Leydig tumor cell genes in response to MEHP dose (A) and MEHP plus hCG stimulation (B). *Rows* represent individual genes, and *columns* represent different treatments: WP-1, WP-3, WP-5, WP-7, and WP-9 represent treatments with 0 (control), 0.3, 1, 3, and 10 μM MEHP, respectively, without hCG stimulation; WP-2, WP-4, WP-6, WP-8, and WP-10 represent treatments with 0, 0.3, 1, 3, and 10 μM MEHP, respectively, and then stimulation with hCG. *Red* indicates high expression, and *green* indicates low expression. Color intensity is based on row-normalized values.

48 h compared with control samples. Supplemental Table 9 summarizes the genes that responded when the cells were exposed to 1 μM MEHP for 48 h, followed by exposure to 50 ng/ml hCG for 2 h. Protein changes are listed with respect to confidence level, with 5 being the highest level of confidence (see legend to Supplemental Table 8). Proteins having multiple bands are presented with observed molecular weights included in their names (Supplemental Tables 8 and 9).

Of the 860 gene products examined by PowerBlot, 26 were differentially expressed relative to controls (above

2-fold difference with high confidence, level 5) in MEHP-treated MA-10 cells (Supplemental Table 8). Eight of the 860 gene products examined by PowerBlot were differentially expressed in MEHP and then hCG-treated MA-10 cells compared with controls exposed only to hCG (Supplemental Table 9). Venn diagrams were used to visualize gene-expression profiles from high-throughput immunoblots after MEHP or MEHP/hCG treatment. This analysis identified 16 and 24 genes that were up- and down-regulated by MEHP and MEHP/hCG treatments, respectively (Supplemental Fig. 4A). Only a small number of genes up- and down-regulated by MEHP alone were found to be reversely regulated by MEH and hCG treatment (Supplemental Fig. 4A). The expression of eight among the selected 11 genes in the list correlated with PowerBlot data (Supplemental Fig. 4B).

Supplemental Table 10 shows a protein information matrix classifying the features of 112 MEHP response genes identified by PowerBlot analysis in MEHP-treated cells without hCG stimulation. As seen in the table, these genes were classified into 14 process categories, 11 pathway clusters, and 50 function categories. One prominent group of gene products that responded to MEHP is involved in cell signaling, cytokine/chemokine, cell activation, cell-cycle regulation, apoptosis, adhesion, and immunology pathways. A second prominent group is involved in cell communication, cell growth, and metabolism process categories. Supplemental Table 11 shows a protein information matrix that summarizes the features of 189 response genes identified by PowerBlot analysis in MEHP-treated MA-10 cells after their stimulation with hCG. The genes were classified into 13 process categories, 11 pathway clusters, and 54 function categories. One large group of these genes is involved in cell signaling, cytokine/chemokine, cell activation, cell-cycle regulation, apoptosis, adhesion, and immunology pathways. A second large group is involved in cell communication, cell growth, and/or maintenance and metabolism categories.
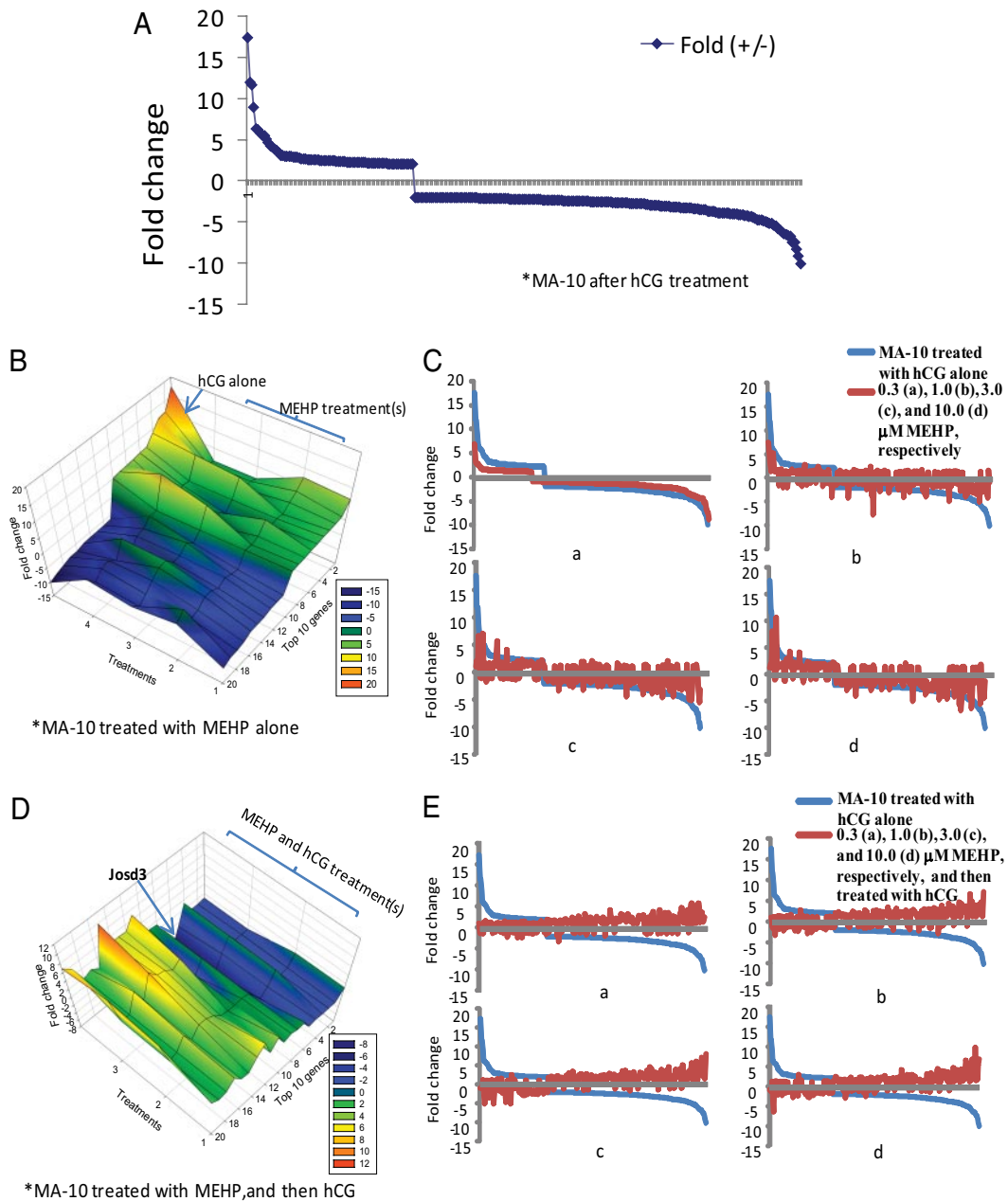
FIG. 3. The effect of MEHP treatment(s) on hCG-responsive genes in MA-10 cells. A, Up- and down-regulation of oxidative stress and steroid biosynthesis genes in cells treated with hCG alone. There were a total of 88 genes with at least 2-fold changes and 188 genes with less than or equal to 2-fold changes. B, The response of the top 10 up- and down-regulated genes (at least 2-fold changes) to hCG compared with MEHP alone. C, The profiling of the hCG-stimulated genes with at least 2-fold changes (a) compared with the profiling of the same set of genes stimulated by MEHP at 0.3 (b), 3.0 (c), or 10.0 (d) μM MEHP. D, The response of the top 10 up- and down-regulated genes to hCG compared with MEHP plus hCG. Josd3, Josephin domain containing 3 or TATA box binding protein (TBP)-associated factor, RNA polymerase I, D (94476_at). E, The profiling of the hCG-stimulated gene set responsive to MEHP/hCG treatments as indicated (a–d).

Comparison of effects of hCG alone, MEHP alone, and hCG plus MEHP on gene expression by MA-10 cells

Figure 3A depicts the 88 genes that increased and the 188 genes that decreased by at least 2-fold in response to hCG stimulation alone. First, the top 10 up- and down-regulated among these genes were selected. Their responses to hCG and to MEPH alone (four concentrations, ranging from 0.3 to 10 μM) are depicted as a three-dimen-

sional mesh plot (Fig. 3B). Observation of this plot suggests similar expression profiling in response to MEHP as to hCG, particularly at a low MEHP concentration. Figure 3C, a–d, depicts the hCG effects on the 276 genes shown in Fig. 3A against the effects of MEHP at 0.3 (Ca), 1.0 (Cb), 3.0 (Cc), and 10.0 (Cd) μM. The genes that responded positively (n = 88) or negatively (n = 188) to hCG responded remarkably similarly to 0.3 μM MEHP alone (Fig. 3Ca). With increasing concentrations of
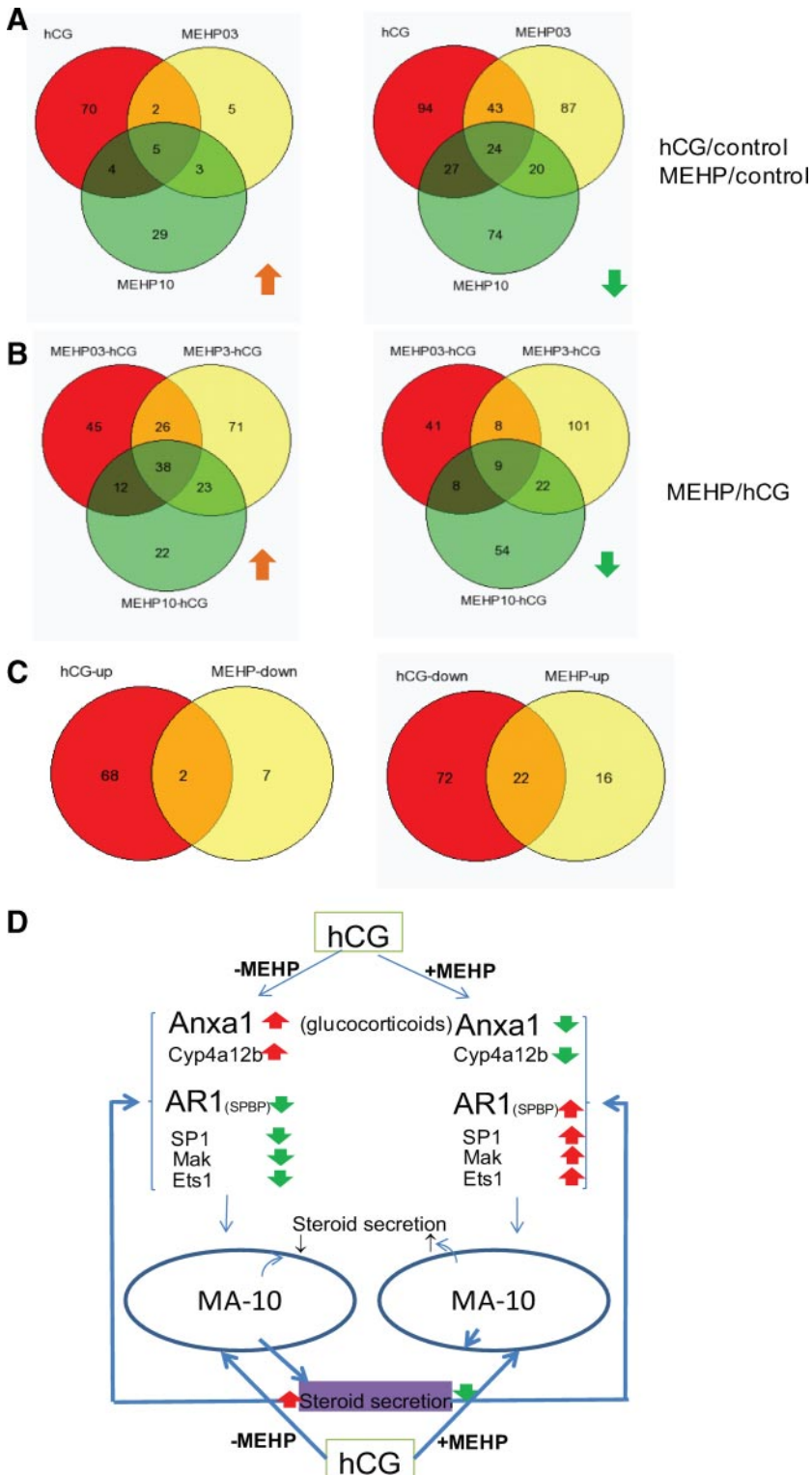
FIG. 4. Venn diagrams depicting differences and commonalities in number of up- and down-regulated genes in response to hCG, MEHP, or MEHP plus hCG. A, Coexpression of genes with at least 2-fold or no more than 2-fold changes by hCG and MEHP over control, respectively. B, Coordinated expression of genes with at least 2-fold or no more than 2-fold changes by three concentrations of MEHP. C, Gene-expression profiles with opposite regulation by hCG and MEHP, respectively. The genes for each of the Venn diagrams are listed in Supplemental Materials and Methods. D, A proposed feedback mechanism of steroidogenesis in MA-10 cells regulated by hCG and MEHP. MAK, Male germ cell-associated kinase.

MEHP (Fig. 3C, b–d), expression profiling remained similar to the expression in response to hCG, although not as much as with low-dose MEHP. In contrast to the similarity between the effects of treatment with MEHP alone and hCG, the expression profiling of the MA-10 cells treated with MEHP plus hCG differed considerably from the effects of treatment with hCG alone, with similar trends for all the MEHP concentrations used (Fig. 3, D and E, a–d).

Comparison of gene regulation between hCG and MEHP reveals a self-regulation mechanisms of steroidogenesis in MA-10 cells

As seen in Venn diagrams (Fig. 4A–C) (for full datasets, see Supplemental Table 12), among the 277 genes significantly changed by hCG (Fig. 3A), five were up-regulated and 24 genes were down-regulated by both hCG and MEHP treatments. Thirty-eight genes were up-regulated by three different concentrations of MEHP, whereas only nine were down-regulated under the same conditions. To cross-compare the gene-expression profiles, we found that two genes were up-regulated by hCG and down-regulated by MEHP, and 22 genes were down-regulated by hCG and up-regulated by MEHP. We suggest that these opposite regulations of gene expression might be linked with a new feedback mechanism of self-regulation of steroidogenesis under stress conditions (Fig. 4D).

One of the two genes up-regulated by hCG and down-regulated by MEHP was *Anxa1*, which has been shown to mimic the inhibitory action of glucocorticoids on testosterone formation (45). The other was *Cyp4a12b*, which is involved in the hydroxylation of arachidonic acid to 20-hydroxyeicosatetraenoic acid and plays a role in vascular and renal tubule function (47), and likely is related to the normal functions of hCG-stimulated steroidogenesis. Among the 22 genes down-regulated by hCG and up-regulated by MEHP, androgen receptor 1 (AR1) is the transcription factor 20, a transcriptional co-activator that enhances the activity of
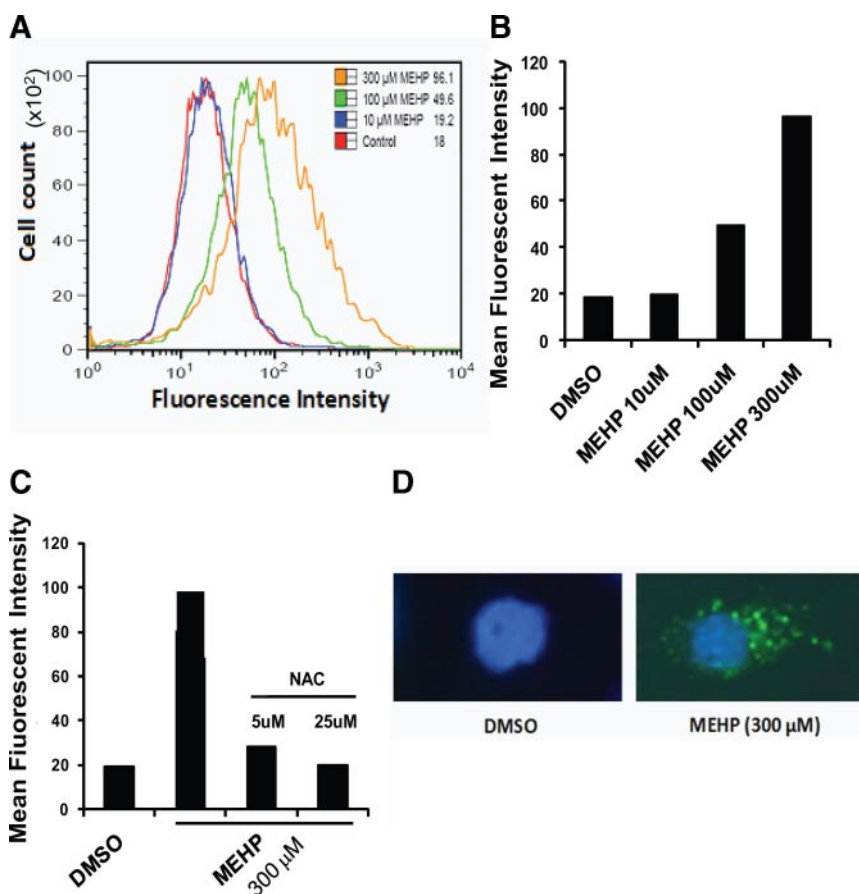
FIG. 5. ROS generation induced by MEHP in MA-10 cells was assessed using the DCFH-DA-dependent fluorescent assay. A, Measurement of the fluorescent dichlorofluorescein oxidized by cellular oxidants from the dichlorofluorescein, which is formed through hydrolysis of DCFH-DA by intracellular esterases. B, Dose-dependent increase of the fluorescence intensity of MA-10 cells treated with MEHP (10–300 μM). C, Effect of the antioxidant NAC on the fluorescence intensity of MA-10 cells treated with 300 μM MEHP. D, Cellular localization of the dichlorofluorescein-derived fluorescence in a representative cell, showing a putative mitochondrial distribution pattern. DMSO, Dimethylsulfoxide.

using the DCFH-DA-dependent fluorescent assay. Incubating MA-10 cells with MEHP (100–300 μM, 2–3 h) increased the fluorescence intensity significantly as a function of MEHP dose, with no effect on cellular toxicity (Fig. 5, A and B). The increase seen even with the highest concentration used (300 μM) was blocked by preincubation of the cells with the antioxidant N-acetylcysteine (NAC), suggesting that ROS were responsible for the fluorescence induced by MEHP (Fig. 5C). Examination of DCFH-DA-derived fluorescence in individual cells by video-capture time-lapse fluorescent microscopy revealed an accumulation in mitochondria (Fig. 5D).

Effect of MEHP on ROS and steroidogenesis pathways

Figure 6 and Supplemental Figs. 5 and 6 show a schematic overview, generated by GenMAPP (38), of the expression profiles of genes involved in selected ROS and steroidogenesis pathways. Fold changes in response to hCG and MEHP treatments are mapped. Genes up-regulated ($\geq$2-fold) by hCG and/or MEHP are coded in *red* or *orange*, whereas genes down-regulated are coded in *blue* or *purple*. In the ROS pathway, it can be seen that the *Cyp1a1* gene was up-regulated by MEHP in hCG-stimulated MA-10 cells, whereas several other genes, such as *junB*, are were regulated by MEHP but to a lesser extent. In the steroidogenesis pathway, *Cyp17a1* was down-regulated by MEHP alone (Supplemental Fig. 5) but up-regulated by MEHP in the hCG-stimulated cells (Fig. 6); several other enzymes involved in steroid synthesis also were down-regulated by MEHP in the hCG-stimulated cells. These changes in gene expression are likely responsible for the reduction of steroidogenesis in response to MEHP (Fig. 1, A and B).

Cyp1a1, besides its role in the detoxification of polycyclic aromatic compounds, has been shown to generate mutagenic metabolites and oxidative stress (52). Many genes involved in its gene network are related to xenobiotic metabolism, such as *Cyp4b1*, and to ROS generation, such as *Acp5* (53, 54). *Cyp1a1* might be the link between xenobiotic metabolism (*Cyp4b1*), endobiotic metabolism (*Cyp17a1*), and ROS generation (*Acp5*) (Fig. 7A). Analysis of the expression profiles after hCG and/or MEHP treatment indicated that many genes of the *Cyp1a1* net-

transcription factors such as *jun* and *Sp1*. These transcription factors are regulated by androgens and synthetic steroids. The mouse version of AR1 is the stromelysin-1 platelet-derived growth factor-responsive element-binding protein, which is a repressor of estrogen receptor α (48). It is noteworthy that one of the few protein kinases associated with AR as a coactivator is male germ cell-associated kinase (49), and one of the AR gene targets is the avian erythroblastosis virus E26 homolog (ETS) transcription factor family (Ets1) (50). Therefore, these data indicate that the expression of AR and associated genes, including some transcription factors, are down-regulated in response to hCG.

MEHP effects on ROS generation

MEHP treatment has been reported to result in the generation of ROS and thus in impairment of mitochondrial function and release of cytochrome *c* in the testis (51). ROS levels in MA-10 cells in response to MEHP were assessed

FIG. 6. Analysis of oxidative stress and steroid biosynthesis pathways in the gene-expression profiles in MA-10 cells treated with MEHP plus hCG. Both oxidative (A) and steroid biosynthesis (B) pathways were overlain with gene expression using the program GenMAPP (version 2.1) and the color criterion and ratios of gene expression used: *orange*, at least 2-fold up-regulation by MEHP; *red*, no more than 2-fold up-regulated by MEHP; *green*, no more than 2-fold down-regulated by MEHP; and *purple*, at least 2-fold down-regulated by MEHP; *gray*, no criteria met; *white*, gene is not present in the Affymetrix Murine Genome U74A version 2 GeneChip or in the mouse GenMAPP database (version June 28, 2006). *Boxes overlain with more than one color* suggest that the gene is covered on the array by multiple hits. C03, C10, C30, and C100 indicate that the cells were treated with 0.3, 1.0, 3.0, and 10.0 μM MEHP plus hCG stimulation, respectively. The number next to each gene indicates the fold change in C100 compared with control in oxidative pathway, whereas the fold change in C03 in steroid biosynthesis pathway is shown. The expression ratio profiling of the gene with the most significant change induced by the treatment together with its four closest neighboring genes (prepared using GenePattern version 3.1.1.) is also shown. Mapk14, MAPK 14; Junb, Jun-B oncogene; Fos, FBJ osteosarcoma oncogene; Nrf2, nuclear factor, erythroid derived 2, like 2; Nfkb1, nuclear factor of κ light chain gene enhancer in B-cells 1, p105; Sp1, trans-acting transcription factor 1; Hmox1, heme oxygenase (decycling) 1; Gpx1, glutathione peroxidase 1; Nqo1, NAD(P)H dehydrogenase quinone 1; Cat, catalase; Txn2, thioredoxin 2; Txnrd1, thioredoxin reductase 1; Txnrd2, thioredoxin reductase 2; Gclc, glutamate-cysteine ligase, catalytic subunit; Mt1, metallothionein 1; Gsr, glutathione reductase 1; Gstt2, glutathione S-transferase θ 2; Mgst1, microsomal glutathione S-transferase 1; Sod1, Superoxide dismutase; Sod2, superoxide dismutase 2 mitochondrial; Sod3, superoxide dismutase 3 extracellular; Nfix, nuclear factor I/X; Cyp1a1, cytochrome P450 family 1 subfamily a, polypeptide 1; Cyba, cytochrome b-245 α polypeptide; Xdh, Xanthine oxidase; Maoa, monoamine oxidase A; Cyp17a1, cytochrome P450 family 17; Hsd3b1, hydroxysteroid dehydrogenase-1 δ-3-β; Hsd3b6, hydroxysteroid dehydrogenase-6 δ-3-β Hsd17b4, hydroxysteroid (17-β) dehydrogenase 4. All pathways used were modified from the GenMAPP pathway. Note that the mineralocorticoids, glucocorticoids, and testosterone shown in the figure are not main steroid products of the MA-10 cell line and are shown herein to visualize the genes relevant to the general steroidogenesis pathway.

work were up-regulated (Fig. 7B). In the presence of low concentrations of MEHP alone, *Cyp1a1* was down-regulated; with relatively low concentrations of MEHP plus hCG treatment or with high concentrations of MEHP alone or in the presence of hCG, *Cyp1a1* was up-regulated. All changes seen were confirmed by Q-PCR (Fig. 7, C and D). These data suggest that the MEHP-induced expression of *Cyp1a1* might be associated with the excess

ROS generated by MEHP in the MA-10 cells and localized in mitochondria, the site in which steroidogenesis begins.

Discussion

The primary goal of the present study was to begin to elucidate the molecular mechanisms by which MEHP ex-
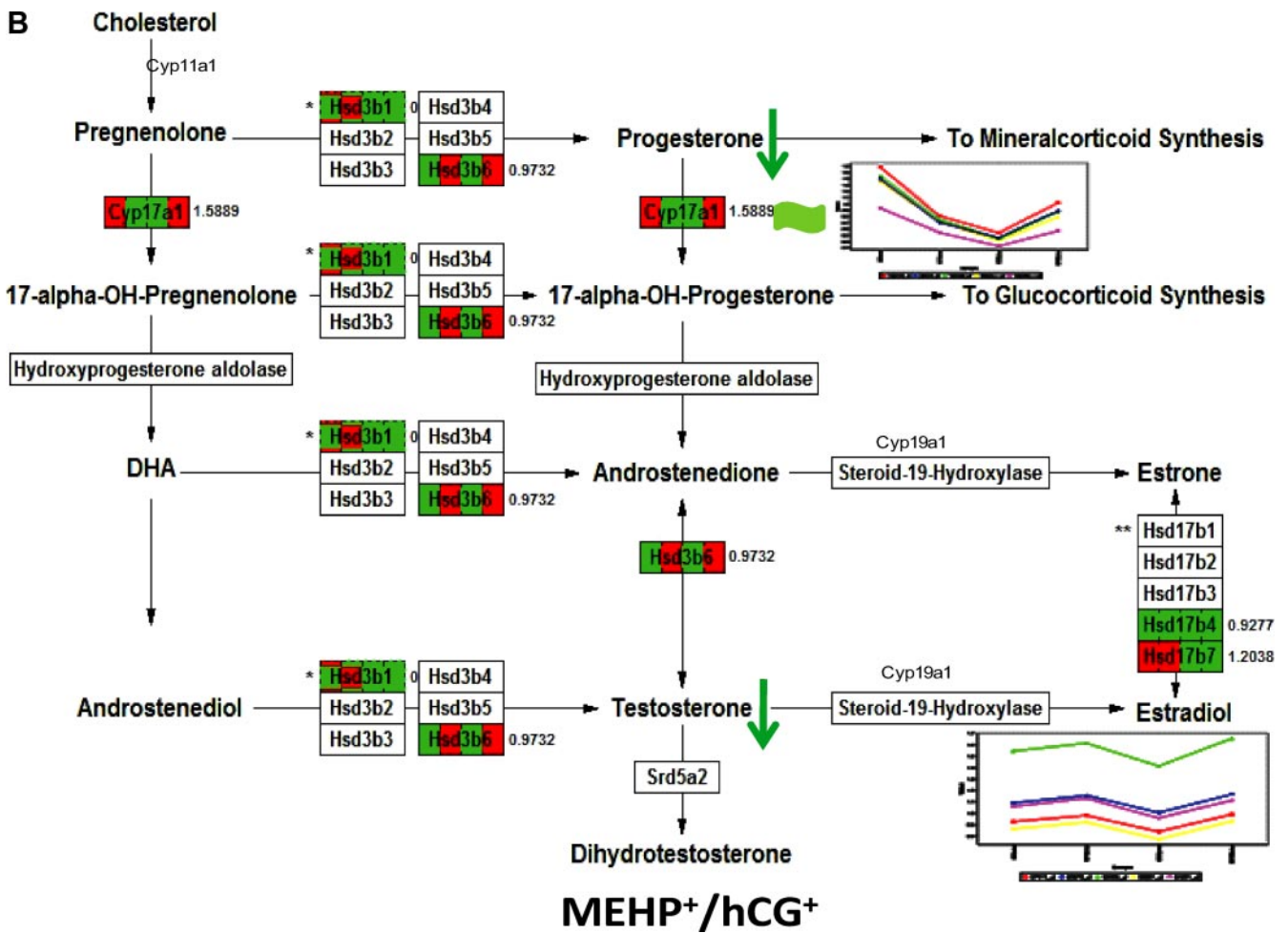
FIG. 6. *Continued.*

posure affects steroid production. Treatment of MA-10 cells with MEHP for 48 h inhibited hCG-stimulated steroid formation significantly, with an IC_{50} value of less than 1 μM, in agreement with previous studies (55). Treatment of isolated rat Leydig cells with MEHP similarly resulted in reduced testosterone production, validating the use of MA-10 cells as a model system for the present studies. Interestingly, whereas treatment of the MA-10 cells with 1–10 μM MEHP resulted in decreased progesterone production, treatment with a relatively low MEHP concentration (0.1 μM) slightly increased steroid synthesis. As discussed below, treatment of MA-10 cells with 0.1 μM MEHP resulted in gene-expression profiling similar to that seen in the presence of hCG alone, which may explain the increase in progesterone production in response to low MEHP concentration.

Along with effects on progesterone production, MEHP treatment of MA-10 cells resulted in significant changes in gene and protein expression. The expression of a number of genes increased in response to MEHP and/or MEHP plus hCG, including *Egr1*, *JunB*, *Nr4a1*, and *P160*, the protein products of each of which are related to carcino-

genic/anticarcinogenic mechanisms. In particular, overexpression of EGR1 stimulates the generation of ROS (55). Thus, the increased expression of the *Egr1* gene induced by MEHP may relate to ROS-mediated carcinogenic/anticarcinogenic mechanisms. A second gene that increased in response to MEHP was *JunB*. This MEHP-induced change is of interest because *JunB*, a major component of the activator protein-1 transcription factor complex, has been shown to control cyclin A during cell-cycle regulation in mouse embryo fibroblasts, indicating that it may be a negative regulator of cell proliferation (56, 57). Thus, its increased expression in response to MEHP could be associated with an anticarcinogenic effect. The expression of a number of genes decreased in response to MEHP exposure, among which were *Clk*, *Dld*, *Msh2*, *Stat6*, *Xpol*, and *Zfp97*. A number of the genes are involved in ROS generation and oxidative stress. For example, *Dld* belongs to electron transport and glycolysis in the biological process category of gene ontology and is located both in mitochondria and cytoplasm. Its molecular functions are dihydrolipoamide dehydrogenase activity, metal ion binding, disulfide oxidoreductase activity, and oxidoreductase
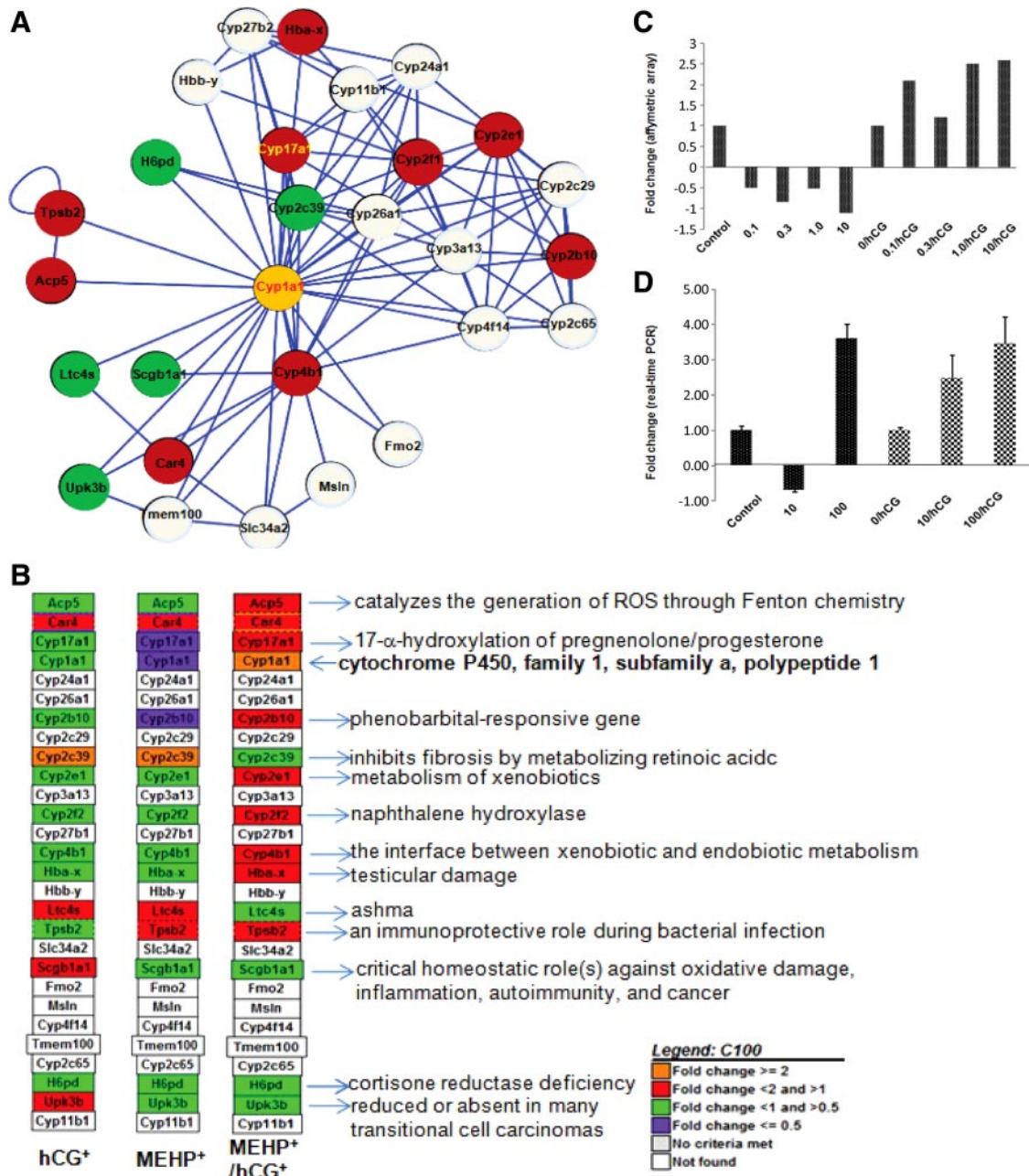
FIG. 7. The gene network of Cyp1a1 and its regulation by MEHP and hCG treatments. A, Gene network of *Cyp1a1*. The gene networks were constructed through the IntNetDB server (http://hanlab.genetics.ac.cn/sys/intnetdb) using *Cyp1a1* (Gene ID no. 13076) as probes. B, Gene list involved in the *Cyp1a1* network generated by GenMAPP. *Red*, Increased expression; *orange*, significantly increased expression (≥2-fold); *green*, decreased expression; *purple*, significantly decreased expression (≥2-fold). *White* indicates that selection criteria were not met but the gene was represented in the array. The references to color in this figure legend are indicated. Different treatments are shown below each of the gene lists. The proposed functions and gene names are indicated beside the gene lists. Acp5, Acid phosphatase 5, tartrate resistant; Car4, carbonic anhydrase 4; Cyp1a1, cytochrome P450, family 1, subfamily a, polypeptide 1; Cyp17a1, cytochrome P450, family 17, subfamily a, polypeptide 1; Cyp24a1, cytochrome P450, family 24, subfamily a, polypeptide 1; Cyp26a1, cytochrome P450, family 26, subfamily a, polypeptide 1; Cyp2b13 (Cyp2b10), cytochrome P450, family 2, subfamily b, polypeptide 13; Cyp2c29, cytochrome P450, family 2, subfamily c, polypeptide 29; Cyp2c39, cytochrome P450, family 2, subfamily c, polypeptide 39; Cyp2e1, cytochrome P450, family 2, subfamily e, polypeptide 1; Cyp3a13, cytochrome P450, family 3, subfamily a, polypeptide 13; Cyp2f2, cytochrome P450, family 2, subfamily f, polypeptide 2; Cyp27b1, cytochrome P450, family 27, subfamily b, polypeptide 1; Cyp4b1, cytochrome P450, family 4, subfamily b, polypeptide 1; Hba-x, hemoglobin X, α-like embryonic chain in Hba complex; Hbb-y, hemoglobin Y, β-like embryonic chain; Ltc4s, leukotriene C4 synthase; Mcpt6 (Tpsb2), mast cell protease 6; Slc34a2, solute carrier family 34 (sodium phosphate), member 2; Scgb1a1, secretoglobin, family 1A, member 1 (uteroglobin); Fmo2, flavin containing monooxygenase 2; Msln, mesothelin; Cyp4f14, cytochrome P450, family 4, subfamily f, polypeptide 14; Tmem100, transmembrane protein 100; Cyp2c65, cytochrome P450, family 2, subfamily c, polypeptide 65; H6pd, hexose-6-phosphate dehydrogenase (glucose 1-dehydrogenase); Upk3b, uroplakin 3B; Cyp11b1, cytochrome P450, family 11, subfamily b, polypeptide 1. C, mRNA expression patterns of *Cyp1a1* gene were detected using the Affymetrix Murine Genome U74A v2 GeneChip. D, mRNA expression patterns of *Cyp1a1* gene were confirmed by real-time Q-PCR normalized to hypoxanthine phosphoribosyltransferase. Results shown are fold changes (means ± sD, n = 3).

activity (58), and it is a component of the mitochondrial pyruvate and α-ketoglutarate dehydrogenase complexes and shown to generate ROS (59, 60). Another down-regulated gene is *Xpo1* (exportin 1 or CRM1, chromosome region maintenance 1). *Xpo1* encodes a nuclear protein essential for proliferation and chromosome region maintenance, mediating leucine-rich nuclear export signal-dependent protein transport (61). It is involved in controlling the localization of cyclin B, MAPK, and MAPK-activated kinase 2 and in exporting the oxidative stress-sensitive transcription factor in yeast, which is localized in nucleus to induce the target genes merely under the repression of *Xpo1* (62, 63). The possible significance of the MEHP-induced decrease in the expression of these genes remains unknown but probably involves regulation of ROS-balance and ROS-target gene expression.

Consistent results were not always obtained by Affymetrix array, PowerBlot (when possible), and Q-PCR. In most cases, however, the data obtained correlated well. It should be noted that PowerBlot analysis allowed for the identification of only a subset (10%) of the genes present in the GeneChip array. Thus, a wealth of consistent data were accumulated that integrates genomic, proteomic, and functional data in MEHP-treated steroidogenic cells. Comparison of all the gene datasets, whole pathways, and gene networks, involving thousands of genes and at least dozen or even more genes at a time, reduces bias, which allows confidence in observing changes in global gene expression by Affymetrix array analysis.

As noted above, low-dose MEHP treatment consistently resulted in somewhat increased steroid formation. This phenomenon has been documented as hormesis, *i.e.* small and large concentrations of a substance have opposite effects, across a broad range of biological models, exposures, and outcomes (64). The mechanisms underlying hormesis are not well understood. The finding that low concentrations of MEHP resulted in the generation of a gene profile similar to that obtained with hCG alone may provide a rational interpretation for the hormetic phenomenon observed. However, high concentrations of MEHP targeting multiple genes are obviously detrimental to Leydig cell function. Additional analyses of the MEHP-targeted genes revealed a previously undisclosed self-regulation mechanism of MA-10 cells via *Anxa1* and *AR1* genes under these stress conditions.

Imbalance between pro-oxidants and antioxidants can lead to the accumulation of oxidative damage to a variety of macromolecules within the cell. Thus, when the levels of ROS overcome the antioxidant capacity of a cell, DNA damage, lipid peroxidation, and protein oxidation can occur. Under normal circumstances, such as aging, the accumulation of oxidative damage is considered to be an

important mechanism underlying progressive decline in the functional efficiency of various cellular processes (65). We report herein that increased ROS production results from MEHP exposure and hypothesize that this may play a role in the inhibition of steroidogenesis. This hypothesis is based on a number of observations. For example, lipid peroxidation would be expected to affect membrane structure and/or fluidity, and virtually every event associated with steroidogenesis is dependent on the integrity of cell membranes (66, 67). Hydrogen peroxide, a common intermediate product of oxidative stress in cells, has been shown to inhibit steroidogenesis (68, 69). Moreover, ROS
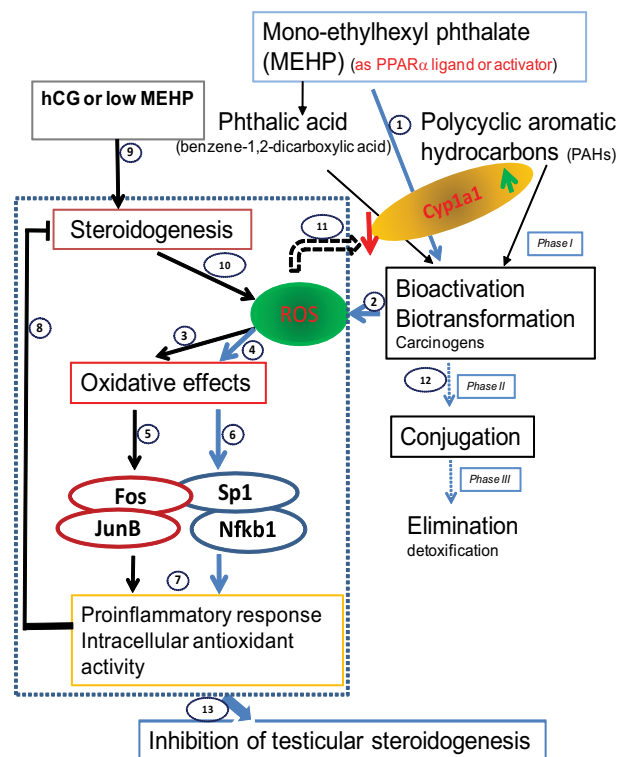
FIG. 8. Mechanism of MEHP-mediated inhibition of testicular steroidogenesis via *Cyp1a1* and ROS. The data suggest that increased ROS caused by changes in the *Cyp1a1* gene disturbs the balance of the steroidogenesis stimulated by hCG, resulting in decreased testicular steroid production. To describe the mechanism in details, each step is highlighted using *dotted circled numbers*. 1, MEHP, a PPARα ligand, activates *Cyp1a1* likely via two peroxisome proliferator response element sites (*green up arrow*) (78); 2, Cyp1a1 generates ROS through the bioactivation/biotransformation of MEHP metabolites; 3 and 4, increased ROS causes oxidative damage; 5 and 6, oxidative effects activate the immediately response genes, Fos/JunB (*circled in red*), and other transcription factors, Sp1/Nfkb1 (*circled in blue*; see also Fig. 3I) (79, 80); 7, the proinflammatory response/intracellular antioxidant activity is the physiological outcome elicited by the activation of these transcription factors; 8, proinflammatory response and oxidant/antioxidant activity causes reduced steroidogenesis (81, 82); 9, hCG or low MEHP stimulates steroidogenesis; 10, ROS is also generated by mitochondrial P450 systems during steroidogenesis (72); 11, the increased ROS decreases *Cyp1a1* expression via feedback regulation system (*red down arrow*) (76); 12, additional metabolized MEHP occurs normally in liver but likely is seen in other cell lines (shown in *dotted line*) (17); 13, the MEHP-induced sequence of events presented above leads to inhibition of steroidogenesis.

can inhibit Leydig cell steroid production (66, 70), and this can be partially prevented by antioxidants (71, 72). Notwithstanding these studies, it is not known whether there is a causal relationship between ROS production and reduced progesterone production by MA-10 cells in response to MEHP. Our previous report indicates that MEHP targets PPARα as a ligand-activated transcription factor, which has proven previously to modulate the oxidant-antioxidant homeostasis in the heart (24, 73). The link between the PPARα and ROS has been missing. Here we provide a model (Fig. 8) to interpret the excesses of ROS generated by MEHP to reduce testicular steroidogenesis through *Cyp1a1* gene and its gene network, which, like many monooxygenases, can produce ROS during its catalytic cycle. *Cyp1a1* directly involves phase I and II xenobiotic metabolism through an oxidative stress-mediated pathway (74, 75). However, the potentially toxic CYP1A1 activity within the cell has been limited through an autoregulatory loop, which leads to the fine tuning of the *Cyp1a1* gene expression through the down-regulation of nuclear factor I activity by *Cyp1a1*-based ROS production (76). Thus, the MEHP-induced expression of *Cyp1a1* might be associated with the excess ROS generated by MEHP in MA-10 cells and localized in mitochondria, the site in which steroidogenesis begins. Steroidogenesis, which involves a number of monooxygenases, also results in ROS production. Thus, accumulated ROS can induce changes in the levels and action of factors, such as Fos, JunB, Sp1, and Nfkb1, that ultimately could block steroid formation (Fig. 8). Comparison of our data on MA-10 cells with a microarray dataset GSE4514 (GenBank) on testis gene expression in rats treated with MEHP revealed that, in both cases, Fos and JunB as well as other genes involved in the ROS pathway are up-regulated by MEHP exposure (77).

In conclusion, the data reported herein have revealed that exposure of MA-10 Leydig cells to MEHP exerts numerous effects on gene expression, protein synthesis, and steroid formation. Among the selected hCG-stimulated genes, high concentrations of MEHP target multiple genes, whereas low MEHP concentration mimics the expression profiles elicited by hCG alone. The latter might explain the mechanism by which low MEHP concentration stimulates steroid synthesis, a hormetic phenomenon. Cross-comparison of the differences and commonalities of gene expression under different treatments revealed that a possible self-regulation of steroidogenesis might exist. In particular, the analysis of ROS and steroid biosynthesis revealed that ROS generated by MEHP affects testicular steroidogenesis via the *Cyp1a1* gene and its gene network. Activation of the PPAR family of transcription factors by MEHP could target the two PPAR response elements in the *Cyp1a1* gene (78). The mechanism by which MEHP acts to inhibit steroidogenesis in MA-10 cells might apply more broadly because a number of endocrine disruptors in the environment generate ROS.

Acknowledgments

References

1. **Fisher JS** 2004 Environmental anti-androgens and male reproductive health: focus on phthalates and testicular dysgenesis syndrome. Reproduction 127:305–315
2. **Forest MG** 1983 Role of androgens in fetal and pubertal development. Horm Res 18:69–83
3. **Gray Jr LE, Kelce WR, Wiese T, Tyl R, Gaido K, Cook J, Klinefelter G, Desaulniers D, Wilson E, Zacharewski T, Waller C, Foster P, Laskey J, Reel J, Giesy J, Laws S, McLachlan J, Breslin W, Cooper R, Di Giulio R, Johnson R, Purdy R, Mihaich E, Safe S, Sonnenschein C, Welshons W, Miller R, McMaster S, Colborn T** 1997 Endocrine screening methods workshop report: detection of estrogenic and androgenic hormonal and antihormonal activity for chemicals that act via receptor or steroidogenic enzyme mechanisms. Reprod Toxicol 11:719–750
4. 1973 Perspective on PAEs. Environ Health Perspect 3:1
5. **Sharman M, Read WA, Castle L, Gilbert J** 1994 Levels of di-(2-ethylhexyl) phthalate and total phthalate esters in milk, cream, butter and cheese. Food Addit Contam 11:375–385
6. **Latini G** 2005 Monitoring phthalate exposure in humans. Clin Chim Acta 361:20–29
7. **Latini G, De Felice C, Presta G, Del Vecchio A, Paris I, Ruggieri F, Mazzeo P** 2003 Exposure to di (2-ethylhexyl) phthalate in humans during pregnancy. A preliminary report. Biol Neonate 83:22–24
8. **Blount BC, Silva MJ, Caudill SP, Needham LL, Pirkle JL, Sampson EJ, Lucier GW, Jackson RJ, Brock JW** 2000 Levels of seven urinary phthalate metabolites in a human reference population. Environ Health Perspect 108:979–982
9. **Duty SM, Silva MJ, Barr DB, Brock JW, Ryan L, Chen Z, Herrick RF, Christiani DC, Hauser R** 2003 Phthalate exposure and human semen parameters. Epidemiology 14:269–277
10. **Main KM, Mortensen GK, Kaleva MM, Boisen KA, Damgaard IN,**

Chellakooty M, Schmidt IM, Suomi AM, Virtanen HE, Petersen DV, Andersson AM, Toppari J, Skakkebaek NE 2006 Human breast milk contamination with phthalates and alterations of endogenous reproductive hormones in infants three months of age. Environ Health Perspect 114:270–276

11. Latini G, De Felice C, Presta G, Del Vecchio A, Paris I, Ruggieri F, Mazzeo P 2003 In utero exposure to di-(2-ethylhexyl) phthalate and duration of human pregnancy. Environ Health Perspect 111:1783–1785

12. Doull J, Cattley R, Elcombe C, Lake BG, Swenberg J, Wilkinson C, Williams G, van Gemert M 1999 A cancer risk assessment of di (2-ethylhexyl) phthalate: application of the new us epa risk assessment guidelines. Regul Toxicol Pharmacol 29:327–357

13. Loff S, Kabs F, Witt K, Sartoris J, Mandl B, Niessen KH, Waag KL 2000 Polyvinylchloride infusion lines expose infants to large amounts of toxic plasticizers. J Pediatr Surg 35:1775–1781

14. Calafat AM, Needham LL, Silva MJ, Lambert G 2004 Exposure to di-(2-ethylhexyl) phthalate among premature neonates in a neonatal intensive care unit. Pediatrics 113:e429–e434

15. Singh AR, Lawrence WH, Autian J 1975 Maternal-fetal transfer of ^{14}C-di-2-ethylhexyl phthalate and ^{14}C-diethyl phthalate in rats. J Pharm Sci 64:1347–1350

16. Calafat AM, Brock JW, Silva MJ, Gray Jr LE, Reidy JA, Barr DB, Needham LL 2006 Urinary and amniotic fluid levels of phthalate monoesters in rats after the oral administration of di (2-ethylhexyl) phthalate and di-n-butyl phthalate. Toxicology 217:22–30

17. Rusyn I, Peters JM, Cunningham ML 2006 Modes of action and species-specific effects of di-(2-ethylhexyl) phthalate in the liver. Crit Rev Toxicol 36:459–479

18. Gray TJ, Gangolli SD 1986 Aspects of the testicular toxicity of phthalate esters. Environ Health Perspect 65:229–235

19. Mylchreest E, Sar M, Cattley RC, Foster PM 1999 Disruption of androgen-regulated male reproductive development by di (n-butyl) phthalate during late gestation in rats is different from flutamide. Toxicol Appl Pharmacol 156:81–95

20. Culty M, Thuillier R, Li W, Wang Y, Martinez-Arguelles DB, Benjamin CG, Triantafilou KM, Zirkin BR, Papadopoulos V 2008 In utero exposure to di-(2-ethylhexyl) phthalate exerts both short-term and long-lasting suppressive effects on testosterone production in the rat. Biol Reprod 78:1018–1028

21. Hurst CH, Waxman DJ 2003 Activation of PPARα and PPARγ by environmental phthalate monoesters. Soc Toxicol 74:297–308

22. Albro PW, Chapin RE, Corbett JT, Schroeder J, Phelps JL 1989 Mono-2-ethylhexyl phthalate, a metabolite of di-(2-ethylhexyl) phthalate, causally linked to testicular atrophy in rats. Toxicol Appl Pharmacol 100:193–200

23. Dees JH, Gazouli M, Papadopoulos V 2001 Effect of mono-ethylhexyl phthalate on MA-10 Leydig tumor cells. Reprod Toxicol 15:171–187

24. Gazouli M, Yao ZX, Boujrad N, Corton JC, Culty M, Papadopoulos V 2002 Effect of peroxisome proliferators on Leydig cell peripheral-type benzodiazepine receptor gene expression, hormone-stimulated cholesterol transport, and steroidogenesis: role of the peroxisome proliferator-activator receptor α. Endocrinology 143:2571–2583

25. Papadopoulos V 2007 Environmental factors that disrupt Leydig cell steroidogenesis. In: Payne AH, Hardy MP, eds. The Leydig cell in health and disease. Totowa, NJ: Humana Press; 393–413

26. Thimmulappa RK, Mai KH, Srisuma S, Kensler TW, Yamamoto M, Biswal S 2002 Identification of Nrf2-regulated genes induced by the chemopreventive agent sulforaphane by oligonucleotide microarray 1. Cancer Res 62:5196–5203

27. Malakhov MP, Kim KI, Malakhova OA, Jacobs BS, Borden EC, Zhang DE 2003 High-throughput Immunoblotting ubiquitin-like protein isg15 modifies key regulators of signal transduction. J Biol Chem 278:16608–16613

28. Papadopoulos V, Mukhin AG, Costa E, Krueger KE 1990 The peripheral-type benzodiazepine receptor is functionally linked to Leydig cell steroidogenesis. J Biol Chem 265:3772–3779

29. Boujrad N, Gaillard JL, Garnier M, Papadopoulos V 1994 Acute action of choriogonadotropin on Leydig tumor cells: induction of a higher affinity benzodiazepine-binding site related to steroid biosynthesis. Endocrinology 135:1576–1583

30. Papadopoulos V, Amri H, Li H, Boujrad N, Vidic B, Garnier M 1997 Targeted disruption of the peripheral-type benzodiazepine receptor gene inhibits steroidogenesis in the R2C Leydig tumor cell line. J Biol Chem 272:32129–32135

31. Castedo M, Ferri KF, Blanco J, Roumier T, Larochette N, Barretina J, Amendola A, Nardacci R, Métivier D, Este JA, Piacentini M, Kroemer G 2001 Human immunodeficiency virus 1 envelope glycoprotein complex-induced apoptosis involves mammalian target of rapamycin/FKBP12-rapamycin-associated protein-mediated p53 phosphorylation. J Exp Med 194:1097–1110

32. Li W, Pretner E, Shen L, Drieu K, Papadopoulos V 2002 Common gene targets of *Ginkgo biloba* extract (EGb 761) in human tumor cells: relation to cell growth. Cell Mol Biol 48:655–662

33. Novak JP, Sladek R, Hudson TJ 2002 Characterization of variability in large-scale gene expression data: implications for study design. Genomics 79:104–113

34. Novak JP, Kim SY, Xu J, Modlich O, Volsky DJ, Honys D, Slonczewski JL, Bell DA, Blattner FR, Blumwald E, Boerma M, Cosio M, Gatalica Z, Hajduch M, Hidalgo J, McInnes RR, Miller 3rd MC, Penkowa M, Rolph MS, Sottosanto J, St-Arnaud R, Szego MJ, Twell D, Wang C 2006 Generalization of DNA microarray dispersion properties: microarray equivalent of t-distribution. Biol Direct 1:27

35. King JY, Ferrara R, Tabibiazar R, Spin JM, Chen MM, Kuchinsky A, Vailaya A, Kincaid R, Tsalenko A, Deng DX, Connolly A, Zhang P, Yang E, Watt C, Yakhini Z, Ben-Dor A, Adler A, Bruhn L, Tsao P, Quertermous T, Ashley EA 2005 Pathway analysis of coronary atherosclerosis. Physiol Genom 23:103–118

36. Sturn A, Quackenbush J, Trajanoski Z 2002 Genesis: cluster analysis of microarray data. Bioinformatics 18:207–208

37. Reich M, Liefeld T, Gould J, Lerner J, Tamayo P, Mesirov JP 2006 GenePattern 2.0. Nat Genet 38:500–501

38. Dahlquist KD, Salomonis N, Vranizan K, Lawlor SC, Conklin BR 2002 GenMAPP, a new tool for viewing and analyzing microarray data on biological pathways. Nat Genet 31:19–20

39. Thayyullathil F, Chathoth S, Hago A, Patel M, Galadari S 2008 Rapid reactive oxygen species (ROS) generation induced by curcumin leads to caspase-dependent and-independent apoptosis in L929 cells. Free Radic Biol Med 45:1403–1412

40. Abate C, Patel L, Rauscher 3rd FJ, Curran T 1990 Redox regulation of Fos and Jun DNA-binding activity *in vitro*. Science 249:1157–1161

41. Andreola F, Hayhurst GP, Luo G, Ferguson SS, Gonzalez FJ, Goldstein JA, De Luca LM 2004 Mouse liver CYP2C39 is a novel retinoic acid 4-hydroxylase: its down-regulation offers a molecular basis for liver retinoid accumulation and fibrosis in aryl hydrocarbon receptor-null mice. J Biol Chem 279:3434–3438

42. Zhu Y, Qi C, Jain S, Le Beau MM, Espinosa 3rd R, Atkins GB, Lazar MA, Yeldandi AV, Rao MS, Reddy JK 1999 Amplification and overexpression of peroxisome proliferatoractivated receptor binding protein (PBP/PPARBP) gene in breast cancer. Proc Natl Acad Sci USA 96:10848–10853

43. Fan J, Wu M, Jiang L, Shen SH 2009 A serine/threonine protein phosphatase-like protein, CaPTC8, from *Candida albicans* defines a new PPM subfamily. Gene 430:64–76

44. Ohinata Y, Sutou S, Kondo M, Takahashi T, Mitsui Y 2002 Male-enhanced antigen-1 gene flanked by two overlapping genes is expressed in late spermatogenesis 1. Biol Reprod 67:1824–1831

45. Cover PO, Baanah-Jones F, John CD, Buckingham JC 2002 Annexin 1 (lipocortin 1) mimics inhibitory effects of glucocorticoids on testosterone secretion and enhances effects of interleukin-1β. Endocrine 18:33–39

46. Perretti M, D'Acquisto F 2009 Annexin A1 and glucocorticoids as effectors of the resolution of inflammation. Nat Rev Immunol 9:62–70

47. **Muller DN, Schmidt C, Barbosa-Sicard E, Wellner M, Gross V, Hercule H, Markovic M, Honeck H, Luft FC, Schunck WH** 2007 Mouse Cyp4a isoforms: enzymatic properties, gender-and strain-specific expression, and role in renal 20-hydroxyeicosatetraenoic acid formation. Biochem J 403:109–118

48. **Gburcik V, Bot N, Maggiolini M, Picard D** 2005 SPBP is a phosphoserine-specific repressor of estrogen receptor α. Mol Cell Biol 25:3421–3430

49. **Ma AH, Xia L, Desai SJ, Boucher DL, Guan Y, Shih HM, Shi XB, deVere White RW, Chen HW, Tepper CG, Kung HJ** 2006 Male germ cell-associated kinase, a male-specific kinase regulated by androgen, is a coactivator of androgen receptor in prostate cancer cells. Cancer Res 66:8439–8447

50. **Massie CE, Adryan B, Barbosa-Morais NL, Lynch AG, Tran MG, Neal DE, Mills IG** 2007 New androgen receptor genomic targets show an interaction with the ETS1 transcription factor. EMBO Rep 8:871–878

51. **Kasahara E, Sato EF, Miyoshi M, Konaka R, Hiramoto K, Sasaki J, Tokuda M, Nakano Y, Inoue M** 2002 Role of oxidative stress in germ cell apoptosis induced by di (2-ethylhexyl) phthalate. Biochem J 365:849–856

52. **Barouki R, Morel Y** 2001 Repression of cytochrome P450 1A1 gene expression by oxidative stress: mechanisms and biological implications. Biochem Pharmacol 61:511–516

53. **Baer BR, Rettie AE** 2006 Cyp4b1: an enigmatic p450 at the interface between xenobiotic and endobiotic metabolism. Drug Metab Rev 38:451–476

54. **Halleen JM, Räisänen SR, Alatalo SL, Väänänen HK** 2003 Potential function for the ROS-generating activity of TRACP. J Bone Miner Res 18:1908–1911

55. **Bek MJ, Reinhardt HC, Fischer KG, Hirsch JR, Hupfer C, Dayal E, Pavenstädt H** 2003 Up-regulation of early growth response gene-1 via the cxcr3 receptor induces reactive oxygen species and inhibits Na$^+$/K$^+$-ATPase activity in an immortalized human proximal tubule cell line 1. J Immunol 170:931–940

56. **Andrecht S, Kolbus A, Hartenstein B, Angel P, Schorpp-Kistner M** 2002 Cell cycle promoting activity of Junb through cyclin a activation. J Biol Chem 277:35961–35968

57. **Shin KH, Kang MK, Kim RH, Christensen R, Park NH** 2006 Heterogeneous nuclear ribonucleoprotein G shows tumor suppressive effect against oral squamous cell carcinoma cells. Clin Cancer Res 12:3222–3228

58. **Liu G, Loraine AE, Shigeta R, Cline M, Cheng J, Valmeekam V, Sun S, Kulp D, Siani-Rose MA** 2003 NetAffx: affymetrix probesets and annotations. Nucleic Acids Res 31:82–86

59. **Starkov AA, Fiskum G, Chinopoulos C, Lorenzo BJ, Browne SE, Patel MS, Beal MF** 2004 Mitochondrial a-ketoglutarate dehydrogenase complex generates reactive oxygen species. J Neurosci 24:7779–7788

60. **Andreyev AY, Kushnareva YE, Starkov AA** 2005 Mitochondrial metabolism of reactive oxygen species. Biochemistry (Mosc) 70:200–214

61. **Kudo N, Khochbin S, Nishi K, Kitano K, Yanagida M, Yoshida M, Horinouchi S** 1997 Molecular cloning and cell cycle-dependent expression of mammalian CRM1, a protein involved in nuclear export of proteins. J Biol Chem 272:29742–29751

62. **Kuge S, Toda T, Iizuka N, Nomoto A** 1998 Crm1 (XpoI) dependent nuclear export of the budding yeast transcription factor yAP-1 is sensitive to oxidative stress. Genes Cells 3:521–532

63. **D'Autréaux B, Toledano MB** 2007 ROS as signalling molecules: mechanisms that generate specificity in ROS homeostasis. Nat Rev Mol Cell Biol 8:813–824

64. **Calabrese EJ, Baldwin LA** 2003 Hormesis: the dose-response revolution. Annu Rev Pharmacol Toxicol 43:175–197

65. **Sohal RS** 2002 Role of oxidative stress and protein oxidation in the aging process. Free Radic Biol Med 33:37–44

66. **Diemer T, Allen JA, Hales KH, Hales DB** 2003 Reactive oxygen disrupts mitochondria in MA-10 tumor leydig cells and inhibits steroidogenic acute regulatory (StAR) protein and steroidogenesis. Endocrinology 144:2882–2891

67. **Edwards PA, Ericsson J** 1999 Sterols and isoprenoids: signaling molecules derived from the cholesterol biosynthetic pathway. Annu Rev Biochem 68:157–185

68. **Behrman HR, Aten RF** 1991 Evidence that hydrogen peroxide blocks hormone-sensitive cholesterol transport into mitochondria of rat luteal cells. Endocrinology 128:2958–2966

69. **Stocco DM, Wells J, Clark BJ** 1993 The effects of hydrogen peroxide on steroidogenesis in mouse Leydig tumor cells. Endocrinology 133:2827–2832

70. **Zirkin BR, Chen H** 2000 Regulation of Leydig cell steroidogenic function during aging. Biol Reprod 63:977–981

71. **Sen Gupta R, Sen Gupta E, Dhakal BK, Thakur AR, Ahnn J** 2004 Vitamin C and vitamin E protect the rat testes from cadmium-induced reactive oxygen species. Mol Cells 17:132–139

72. **Hanukoglu I** 2006 Antioxidant protective mechanisms against reactive oxygen species (ROS) generated by mitochondrial p450 systems in steroidogenic cells. Drug Metab Rev 38:171–196

73. **Schulz R, Ali MA** 2007 PPARα: essential component to prevent myocardial oxidative stress? Am J Physiol Heart Circ Physiol 293:H11–H112

74. **Ross D, Kepa JK, Winski SL, Beall HD, Anwar A, Siegel D** 2000 NAD(P)H: quinone oxidoreductase 1 (NQO1): chemoprotection, bioactivation, gene regulation and genetic polymorphisms. Chem-Biol Interact 129:77–97

75. **Schlezinger JJ, Struntz WD, Goldstone JV, Stegeman JJ** 2006 Uncoupling of cytochrome P450 1A and stimulation of reactive oxygen species production by co-planar polychlorinated biphenyl congeners. Aquat Toxicol 77:422–432

76. **Morel Y, Mermod N, Barouki R** 1999 An autoregulatory loop controlling *CYP1A1* gene expression: role of H$_2$O$_2$ and NFI. Mol Cell Biol 19:6825–6832

77. **Lahousse SA, Wallace DG, Liu D, Gaido KW, Johnson KJ** 2006 Testicular gene expression profiling following prepubertal rat mono-(2-ethylhexyl) phthalate exposure suggests a common initial genetic response at fetal and prepubertal ages. Toxicol Sci 93:369–381

78. **Sérée E, Villard PH, Pascussi JM, Pineau T, Maurel P, Nguyen QB, Fallone F, Martin PM, Champion S, Lacarelle B, Savouret JF, Barra Y** 2004 Evidence for a new human CYP1A1 regulation pathway involving PPAR-α and 2 PPRE sites. Gastroenterology 127:1436–1445

79. **Curran T, Franza Jr BR** 1988 Fos and Jun: the AP-1 connection. Cell 55:395–397

80. **Morel Y, Barouki R** 1999 Repression of gene expression by oxidative stress. Biochem J 342:481–496

81. **Hong CY, Park JH, Ahn RS, Im SY, Choi HS, Soh J, Mellon SH, Lee K** 2004 Molecular mechanism of suppression of testicular steroidogenesis by proinflammatory cytokine tumor necrosis factor α. Mol Cell Biol 24:2593–2604

82. **Chen H, Pechenino AS, Liu J, Beattie MC, Brown TR, Zirkin BR** 2008 Effect of glutathione depletion on Leydig cell steroidogenesis in young and old brown Norway rats. Endocrinology 149:2612–2619